

## Critical Load of Thin-Walled Rod with Various Cross Section Shape by Length

<sup>1</sup>L.S. Sabitov, <sup>2</sup>I.L. Kuznetsov, <sup>2</sup>A.U. Bogdanovich and <sup>2</sup>D.M. Husainov

<sup>1</sup>Kazan State Power Engineering University, Krasnoselskaya Str. 51, Kazan, Russia

<sup>2</sup>Kazan State Architectural University, Zelenaya Str. 1, Kazan, Russia

**Abstract:** The compressed rods of lattice structures are considered with a variable cross-section shape along length at a constant cross section area. The formula of the critical load buckling, differing from Euler's formula by the presence the coefficient which takes into account the changes of inertia moments along a rod length.

**Key words:** Lattice structures, compressed rod of a lattice, a variable cross-section shape at a constant area, the formula of buckling critical force, Russia

### INTRODUCTION

During the design of lattice structures such as farms, frames, power line supports and the structural components for power engineering objects (Kopylov *et al.*, 2015; Reshetnikov *et al.*, 2015; Safin *et al.*, 2015; Misbakhov and Moskalenko, 2015; Misbakhov *et al.*, 2015a, b; Laptev *et al.*, 2015; Gatiyatov *et al.*, 2015; Sabitov *et al.*, 2015) the rolling and cold-formed profiles are used with a constant length of cross-section area length. Using the abovementioned profiles creates the obstacles for lattice structure rod connection components requiring the use of node gusset plates or epy gauge cutting of connected element ends (Yang and Lubinski, 1974). In (Kuznetsov *et al.*, 1991, 2000; Kahn, 1966) the lattice structures are considered which offer the rods with various shape by length and a constant cross-section area as lattice rods (Fig. 1).

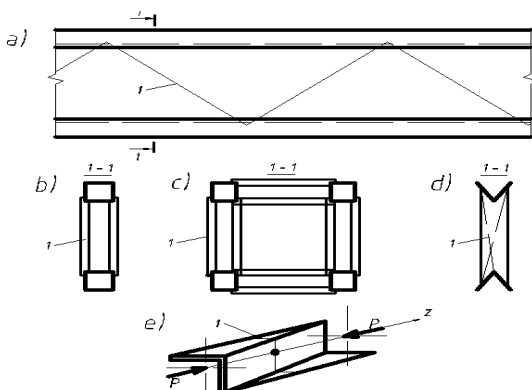


Fig. 1: Latticework scheme a) lattice element (1) of a variable along the section length (e); b) plane lattice structure with the belts of square pipes; c) another spatial latticework; d) flat lattice structure with the belts made of corners

### MATERIALS AND METHODS

**Problem statement:** Let's consider a thin-walled rod Fig. 1 a-e manufactured from a steel strip section by the bending of two parallel lines. This rod is angled at the ends of the profile flanges reverse orientation. The rod is convenient to use as a brace in the lattice structure, as provided by its easy connection with lap bars "in girth" no fancy cutting Fig. 1b, e, d. The rod has a straight central axis Z, a constant cross-sectional area (Table 1) but its other geometrical characteristics are variable, as the section form. The works (Kuznetsov *et al.*, 1998, 1988) provide the equations of bending with the torsion for the bars of a similar type at longitudinal compression with the assumption of possible small initial irregularities and eccentricities. The equations were derived according to Timoshenko (1971) scheme, taking into account the variabilities of all geometric characteristics along axis Z and have the following form:

$$k_1 \varphi^{IV} + k_2 \varphi''' + k_3 \varphi'' + k_4 \varphi' + k_5 \varphi + k_6 v'' + k_7 u' = 0 \quad (1)$$

$$k_8 u'' + k_9 u + k_{10} \varphi = k_9 e_x \quad (2)$$

$$k_{11} v'' + k_{12} v + k_{13} \varphi = k_{12} e_y \quad (3)$$

In Eq. 1-3, the differentiation is performed by z; variable coefficients  $k_i(z)$  are the following ones:

$$k_1 = C_1 = EJ_\omega; \quad k_2 = C_1'(z); \quad C = \frac{1}{3} G \sum_k b_k h_k^3 (+10\%)$$

$$k_3 = -C - p(2y_0 e_y + 2x_0 e_x - x_0^2 - y_0^2 + 2e_x R_y + 2e_y R_x - J_x / F - J_y / F)$$

$$k_4 = -C' - 2p(x_0' e_x + y_0' e_y - x_0 x_0' - y_0 y_0') + 2p\alpha'(x_0 e_y - y_0 e_x)$$

Table 1: Change of rod cross section

Z	F	X <sub>c</sub>	Y <sub>c</sub>	I <sub>o</sub>	I <sub>x</sub>	I <sub>y</sub>	A (mpa)	I <sub>min</sub>
-50	3.2	-1.00	+1.00	0.0000	2.155	8.555	-45.000	0.812
-37.5	3.2	-0.75	+0.75	0.2084	1.862	8.848	-33.185	0.763
-25	3.2	-0.50	+0.50	1.4091	1.355	9.355	-26.565	0.651
-12.5	3.2	-0.25	+0.25	3.7823	0.968	9.741	-23.424	0.550
00.0	3.2	0.00	0.00	5.3352	0.829	9.880	-22.500	0.509
+12.5	3.2	+0.25	-0.25	3.7823	0.968	9.741	-23.424	0.550
+25.0	3.2	+0.50	-0.50	1.4091	1.355	9.355	-26.565	0.651
+37.5	3.2	+0.75	-0.75	0.2084	1.862	8.848	-33.185	0.763
+50.0	3.2	+1.00	-1.00	0.0000	2.155	8.555	-45.000	0.821

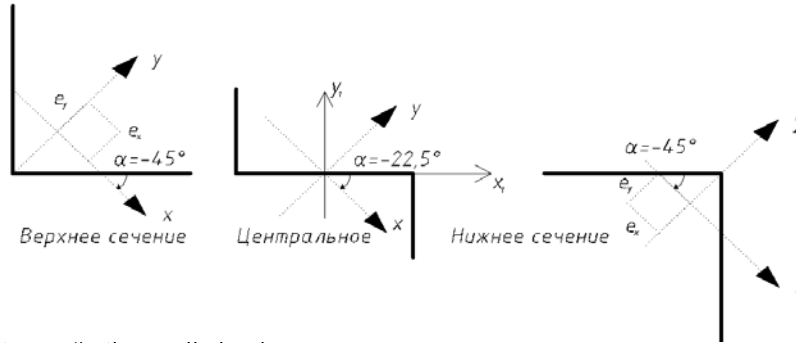


Fig. 2: Cross sections of a thin-walled rod

$$\begin{aligned}
 k_5 &= -p(x_0^* e_x + y_0^* e_y - x_0 x_0^* - y_0 y_0^*) + (\alpha')^2 p(y_0 e_y - x_0 e_x) \\
 &- (\alpha')^2 \frac{P}{F} (J_x + J_y) + \alpha'' p(x_0 e_y - y_0 e_x) \\
 k_6 &= -p(x_0 - e_x), k_7 = -p(e_y - y_0), k_8 = EJ_y(z), k_9 = p \\
 k_{10} &= -p(y_0 - e_y), k_{11} = EJ_x(z), k_{12} = p, k_{13} = p(e_x - x_0) \\
 R_x &= \frac{1}{2J_x} \iint_F y(x^2 + y^2) dF, R_y = \frac{1}{2J_y} \iint_F x(x^2 + y^2) dF
 \end{aligned}
 \tag{4}$$

Where:

- O(x<sub>0</sub>, y<sub>0</sub>) = The shift center (torsion) in the principal central axes of the cross section
- e<sub>x</sub>, e<sub>y</sub> = The eccentricities of a positive compressive force p they may vary in various sections due to an unequal position of the axes x, y, u, v the movement of the point O along the axes x, y, φ torsion angle
- E, G = Material elasticity constants
- b<sub>k</sub>, h<sub>kr</sub> = The dimensions of rectangular cross-section parts
- J<sub>xy</sub>, J<sub>y</sub>, J<sub>o</sub> = The sectorial and axial moments of section inertia
- F = Section area

The orientation of x, y, z axis is shown on Fig. 1 and 2; α(z)-x, y axis inclination angle Fig. 2. Equation 1-3 is the generalization of Kappus-Tymoshenko-Vlasov's equations with the same well-known disadvantages: they do not take into account the geometric nonlinearity at the compression of flexible rods with eccentricity and require

additional analysis at the presence of plastic deformations in the case of rod calculation with an average flexibility. In this study these issues are not addressed.

**Geometric characteristics of weakly twisted rod with variable cross-section:** It is known that the loss of thin rod stability is associated in most cases with the simultaneous bending in two planes and twisting. However, very often the contribution of displacements u, v, φ in this process is not the same, especially when the principal bending stiffness of the rod are very different.

Table 1 shows the change of a rod cross section geometric characteristics along the axis Z for the following option: the corners at the ends 40×40×4 mm; the length l = 100 cm. Table indicated the following: x<sub>c</sub>, y<sub>c</sub> the center of gravity coordinates for each section in the system x<sub>1</sub>, y<sub>1</sub>, agreed with the central section (Fig. 2); J<sub>x</sub>, J<sub>y</sub>, in the main local central axes of each section.

On the upper end (Fig. 1); α-x, y axis inclination angle in each section. All the data of Table 1 in cm and cm powers. Table 1 shows that during the transition from the upper end to the central section the principal axes rotate at 22.5° and then at the transition to the lower end, they return to the initial position.

## RESULTS AND DISCUSSION

**Numerical calculation of thin-walled rod using computer:** The maximum rotation from the principal axes of the central section makes α = 22.50° on the ends. The value J<sub>x</sub> and in each section the displacement v will be

Table 2: Numerical calculations of same rod

P	u×10 <sup>5</sup>	v×10 <sup>5</sup>	φ×10 <sup>7</sup>	det×10 <sup>-24</sup>
80	-0.0500	-0.4705	-0.0029	-0.8735
400	-0.2542	-2.816	-0.0849	-0.8704
720	-0.4656	-6.306	-0.3393	-0.7998
1040	-0.6845	-12.03	-0.9258	-0.6718
1360	-0.9111	-23.14	-2.300	-0.4962
1680	-1.144	-53.71	-6.508	-0.2819
2000	-1.342	-512.21	-72.77	-0.0371
2045.76	+98.51	-0.96·106	-0.14·106	-0.20·10-4
2046.08	-9.898	+0.81·105	+0.12·105	+0.24·10-3

significantly greater than the displacement u. This is confirmed by computer data. Let's name the equation systems Eq. 1-3 conditionally accurate. Table 2 presents the results of numerical calculation using the computer of the same rod, loaded with the eccentricities at the ends of e<sub>x</sub> = e<sub>y</sub> = 0.0001 cm (Fig. 2). By the change of values e<sub>x</sub> and e<sub>y</sub> because of the axes rotation in the intermediate sections at the angle of α = 22.5° (Fig. 2) we neglect it, because of a small eccentricity. Initial parameters: the angle 40×40×4 mm; the length l = 100 cm; e<sub>x</sub> = e<sub>y</sub> = 0.0001 cm; E=2×106 kgf cm<sup>-2</sup>; μ = 0.3; G = E/[2(1+μ)]; the securing of the ends corresponds to the following terms:

$$u = u' = 0; v = v' = 0; \varphi = \varphi' = 0 \tag{5}$$

u, v, φ in Table 2 maximum values of these functions; det to determine the algebraic system of linear equations corresponding to Eq. 1-5 after the problem sampling. Quantity dimension in Table 2: kg, cm, rad. The value of the force p = 2045.76 kgf, after which det changes the sign should be recognized as a critical one.

**Critical load formulae:** Let's consider the central compression case e<sub>x</sub> = e<sub>y</sub> = 0. We have a certain understanding about the mutual relative orders of the value u, v, φ from Table 2. In the Eq. 1-3 we get the following evaluations at any load value:

$$u' \gg \frac{k_{10}}{k_8} \varphi = \frac{y_0 p}{E J_y} \varphi; v' \gg \frac{k_{13}}{k_{11}} \varphi = \frac{x_0 p}{E J_x} \varphi \tag{6}$$

at the evaluation of the equation elements in the vicinity of the ends (Table 1 and 2) it should be borne in mind that:

$$u \approx v \approx \varphi \approx u' \approx v' \approx \varphi' = 0$$

Then, the equations for u, v, φ are divided. At that the critical load determined from the equation for u, will be clearly excessive because of a high bending stiffness in the respective directions of cross sections. The equation for the angle φ in this problem also provides the critical load apparently which is no less than the equations for v,

the solution of which is in a good agreement with the exact solution of the complete system 1-3 in a wide range of lengths and flexibilities. Let's put down Eq. 3 taking into account the evaluations Eq. 6 in the following form:

$$B(z) v''(z) + p v(z) = 0; [B(z) = E J_x(z)] \tag{7}$$

which corresponds to the bending u = φ = 0 in each section. In a good accordance with Table 1, we assume that:

$$B(z) = a_0 + a_1 z^2 \tag{8}$$

Denoting:

$$B_1 = B_{z=-l/2}, B_2 = B_{z=0}$$

we get:

$$a_0 = B_2, a_1 = 4(B_1 - B_2)/l^2 \tag{9}$$

and Eq. 7 takes the following form:

$$(a_0 + a_1 z^2) v''(z) + p v(z) = 0 \tag{10}$$

Let's take collocation method. Let

$$v(z) = b_1 \cos\left(\frac{\pi z}{l}\right) + b_2 \cos\left(\frac{3\pi z}{l}\right) \tag{11}$$

taking into account the first two harmonics of the movement v(z). In this case, the boundary conditions (Eq. 3) and the Eq. 10 at z = -l/4 and z = 0 we obtain the system of two linear equations

$$\begin{aligned} b_1(p - C_1) + b_2(p - C_2) &= 0 \\ b_1(p - C_3) + b_2(-p + C_4) &= 0 \end{aligned} \tag{12}$$

Where:

$$\begin{aligned} C_1 &= a_0(\pi/l)^2 \\ C_2 &= a_0(3\pi/l)^2 \\ C_3 &= (a_0 + a_1 l^2/16)(\pi/l)^2 \\ C_4 &= (a_0 + a_1 l^2/16)(3\pi/l)^2 \end{aligned}$$

From the system determinant Eq. 12 equal to zero, we obtain the following:

$$p^2 - p 5(\pi/l)^2 (2a_0 + a_1 l^2/16)(\pi/l)^4 \tag{13}$$

From which taking into account Eq. 9:

$$p_{kp} = \left(\frac{\pi}{l}\right)^2 E J_x^{(2)} \gamma \tag{14}$$

Where:

$$\gamma = \frac{5}{8}(7+\beta) \left[ 1 \pm \frac{144}{25}(3+\beta)/(7+\beta)^2 \right] \quad (15)$$

$$\beta = \frac{B_1}{B_2} = J_x^{(1)}/J_x^{(2)}; J_x^{(1)} = J_x \Big|_{z=\pm l/2}; J_x^{(2)} = J_x \Big|_{z=0} \quad (16)$$

At all  $\beta > 0$  the radical expression in Eq. 15 is a positive one and the Eq. 13 has 2 real positive roots, the smaller of which provides the first critical load Eq. 14 with the sign (-) in Eq. 11. For the constant section rod  $Ej_x(z) = \text{const}$ ;  $a_1 = 0$ ;  $\beta = 1$ ;  $\gamma = 1$ . Then according to the Eq. 14 we obtain the following:  $p_{Kp} = (\pi-1)^2 \cdot Ej_x$  which corresponds to Euler's formula for a constant section rod. The second root of the Eq. 13 in this case is nine times greater and corresponds to the second harmonic of the Eq. 11. Let's compare the solution Eq. 14 with the numerical solution of the problem 1-3, 5 using a computer for a variety of flexibilities. Let's introduce the conditional (secondary) flexibility:

$$\lambda_p = \mu_0 l / i_{\min}^p; \mu_0 = 1; i_{\min}^p = \frac{1}{k} \sum_k i_{\min}^{(k)} \quad (17)$$

where,  $i_{\min}^{(k)}$  are taken from Table 1 (Table 1 values depend on section values and the length  $l$ ). Let's emphasize that at the derivation of the Eq. 14, the average flexibility was not used and even its concept was not introduced. Fig. 3:

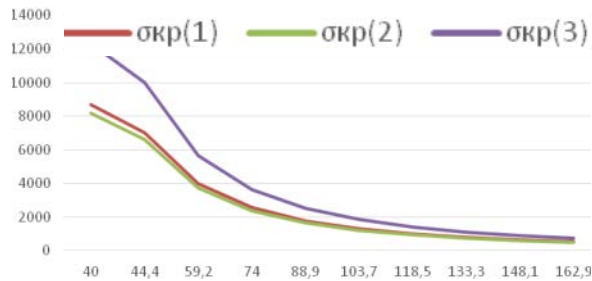


Fig 3: The graphs of durability dependence on flexibility

Table 3: Critical external compression stress

$\lambda_{cp}$	$\sigma_{Kp}^{(1)}$	$\sigma_{Kp}^{(2)}$	$\sigma(1,2)\%$	$\sigma_{Kp}^{(3)}$	$\sigma(1,3)\%$
40.0	8662.6	8156.5	-5.84	12337.0	42.4
44.4	7033.2	6606.8	-6.06	10013.0	42.4
59.2	3974.5	3716.3	-6.50	5632.2	41.7
74.0	2549.4	2378.4	-6.71	3604.6	41.4
88.9	1772.6	1651.7	-6.82	2497.6	40.9
103.7	1303.3	1213.5	-6.89	1835.6	40.8
118.5	998.3	929.1	-6.93	1405.7	40.8
133.3	789.0	734.1	-6.96	1110.9	40.8
148.1	639.3	594.6	-6.99	899.9	40.8
162.9	528.4	491.4	-7.00	743.8	40.8

shows the values of the critical external compressive stresses:  $\sigma_{Kp}^{(1)}$  "exact solution";  $\sigma_{Kp}^{(2)}$  the solution according to the Eq. 14; in both cases  $\sigma_{Kp} = p_{Kp}/F$  ( $F = \text{const}$ ).

The calculations were performed for different variants of end corners and the length  $l$ . The curves  $\sigma_{Kp}^{(1)}(\lambda_{Kp})$  were absolutely identical in all variants; the curves  $\sigma_{Kp}^{(2)}(\lambda_{cp})$  were also identical. This result is important and was not obvious beforehand. Sometimes they make attempts to solve such problems by substituting some average flexibility in Euler's formula. Figure 3 shows the values of  $\sigma_{Kp}^{(3)} = \pi^2 E / \lambda_{cp}^2$  where  $\lambda_{cp}$  Eq. 16 was taken. The exact values  $\sigma_{Kp}$  (kgf/cm<sup>2</sup>) and errors

$$\delta_{(1,3)} \% = 100\% \cdot [\sigma_{Kp}^{(3)} - \sigma_{Kp}^{(1)}] / \sigma_{Kp}^{(1)}$$

$$\delta_{(1,2)} \% = 100\% \cdot [\sigma_{Kp}^{(2)} - \sigma_{Kp}^{(1)}] / \sigma_{Kp}^{(1)}$$

Are presented in Table 3. The following follows from Fig. 3: at  $\lambda_{Kp} = 40$  the Eq. 14 adequately reflects the essence of the considered buckling process with a little underestimation of the values  $p_{Kp}$  or  $\sigma_{Kp}$  in stability margin (no >7%). The study of the Eq. 14 for the sections of other variables may change if the section shape changes smoothly and the table of  $J_{\min}$  values is symmetrical in respect of a single extremum in the center. In any case a preliminary deep analysis of a problem is required. As for the stresses  $\sigma_{Kp}^{(3)} = \pi^2 E / \lambda_{cp}^2$  on Fig. 3 they are far from exact values. However, introducing an empirical correction factor, we obtain the formula which provides the critical stresses close to  $\sigma_{Kp}^{(1)}$  with a maximum error of no >1.2% for area decrease Eq. 14:

$$\sigma_{Kp}^{(4)} = \frac{\pi^2 E}{\lambda_{cp}^2} \gamma_1 \quad (18)$$

$$\lambda_1 = 0.70175 \quad (19)$$

### CONCLUSION

On the basis of the above mentioned information one may conclude that the proposed formulas allow their use in the practice of lattice structure design which have a good agreement with the known procedures obtained by computer. The formulae for the critical load determination were obtained for the proposed new structural forms of lattice structures made of steel thin-walled formed sections. The scientific novelty and the practical effectiveness of these rods is confirmed by the invention

patents but their use and their introduction into production was held back so far by the lack of a theoretical base for the calculation of such rods stability.

#### ACKNOWLEDGEMENTS

The research was supported by the Assistance Fund for Small Innovative Enterprises in Science and Technology.

#### REFERENCES

- Gatiyatov, I., I. Kuznetsov, L. Sabitov and L. Ibragimov, 2015. Deflected mode of junction of pipes of different diameters in the constructions of contact-line supports of electrical transport. *Int. J. Applied Eng. Res.*, 10: 45255-45263.
- Kahn, S.N., 1966. *Construction Mechanics of Shells*. Engineering Press, Moscow, Russia, Pages: 504.
- Kopylov, A.M., I.V. Ivshin, A.R. Safin, R.S. Miesbachov and R.R. Gibadullin, 2015. Assessment, calculation and choice of design data for reversible reciprocating electric machine. *Int. J. Applied Eng. Res.*, 10: 31449-31462.
- Kuznetsov, I.L., A.E. Gonick and A.F. Salimov, 1991. Lattice structure. AS No. 1684446 MPK E04C3/04, Bulletin No. 38, October 15, 1991.
- Kuznetsov, I.L., A.U. Bogdanovich and D.G. Zaynullin, 1988. About the calculation of thin-walled rod stability with variable sections. *Proceedings of the International Conference on Numerical and Analytical Methods of Structure Calculation, (NAMSC'88)*, Samara State Architectural Building Academy, Samara, Russia, pp: 111-113.
- Kuznetsov, I.L., A.U. Bogdanovich and D.G. Zaynullin, 1998. Stability of a thin-walled rod of variable section. *Proceedings of the International Conference of the Reliability and Durability of Building Materials and Structures, (RDBMS'98)*, Volgograd State Architectural Building Academy, Volgograd, Russia, pp: 94-97.
- Kuznetsov, I.L., A.U. Bogdanovich and D.G. Zaynullin, 2000. Latticework made of bent profiles. RF Patent No. 2159310 MPK E04C3/08, Bulletin No. 32, November 20, 2000.
- Laptev, A.G., R.S. Misbakhov and E.A. Lapteva, 2015. Numerical simulation of mass transfer in the liquid phase of the bubble layer of a thermal deaerator. *Thermal Eng.*, 62: 911-915.
- Misbakhov, R. and N. Moskalenko, 2015. Simulation of heat transfer and fluid dynamics processes in shell-and-pipe heat exchange devices with segmental and helix baffles in a casing. *Biosci. Biotechnol. Res. Asia*, 12: 563-569.
- Misbakhov, R.S., V.M. Gureev, N.I. Moskalenko, A.M. Ermakov and I.Z. Bagautdinov, 2015a. Simulation of surface intensification of heat exchange in shell-and-pipe and heat exchanging devices. *Biosci. Biotechnol. Res. Asia*, 12: 517-525.
- Misbakhov, R.S., V.M. Gureev, N.I. Moskalenko, A.M. Ermakov, N.I. Moskalenko and I.Z. Bagautdinov, 2015b. Numerical studies into hydrodynamics and heat exchange in heat exchangers using helical square and oval tubes. *Biosci. Biotechnol. Res. Asia*, 12: 719-724.
- Reshetnikov, A.P., I.V. Ivshin, N.V. Denisova, A.R. Safin, R.S. Misbakhov and A.M. Kopylov, 2015. Optimization of reciprocating linear generator parameters. *Int. J. Applied Eng. Res.*, 10: 31403-31414.
- Sabitov, L., I. Khamidulin, I. Kuznetsov and D. Khusanov, 2015. Stress-strained state of supports for energy construction. *Int. J. Applied Eng. Res.*, 10: 45438-45448.
- Safin, A.R., I.V. Ivshin, A.M. Kopylov, R. Misbakhov and A.N. Tsvetkov, 2015. Selection and justification of design parameters for reversible reciprocating electric machine. *Int. J. Applied Eng. Res.*, 10: 31427-31440.
- Tymoshenko, S.P., 1971. *The Stability of Rods, Plates and Shells*. Nauka, Moscow, Russia, Pages: 708.
- Yang, B. and M. Lubinski, 1974. *Lightweight Steel Structures* (Edited by S.S. Karmilov). Stroyizdat, Moscow, Russia, Pages: 342.